

Absolute Configuration of 3,3'-Diphenyl-[2,2'-binaphthalene]-1,1'-diol Revisited

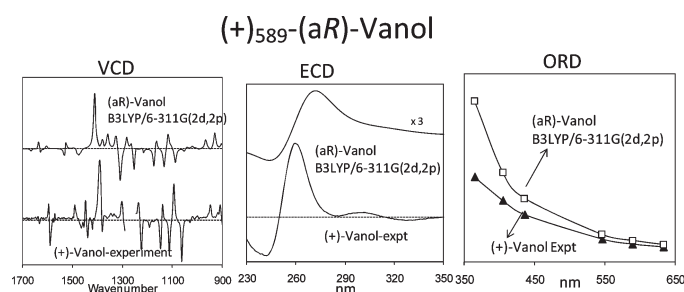
Prasad L. Polavarapu,^{*,†} Ana G. Petrovic,[†] Sarah E. Vick,[†] William D. Wulff,[‡]
Hong Ren,[‡] Zhensheng Ding,[‡] and Richard J. Staples[‡]

[†]Department of Chemistry, Vanderbilt University, Nashville, Tennessee 37235, and

[‡]Department of Chemistry, Michigan State University, East Lansing, Michigan 48824

Prasad.L.Polavarapu@vanderbilt.edu

Received May 14, 2009



The experimental vibrational circular dichroism, electronic circular dichroism, and optical rotatory dispersion spectra and corresponding quantum chemical predictions of 3,3'-diphenyl-[2,2'-binaphthalene]-1,1'-diol (VANOL) are used to confirm its absolute configuration as (+)₅₈₉-(aR) or (-)₅₈₉-(aS). A discrepancy in the literature crystal structure has been resolved by determining the X-ray crystal structure of the brucine binaphtholphosphate salt of the (aS)-enantiomer of VANOL.

Introduction

Substituted enantiomeric 1,1'-bi-2-naphthol compounds have been usefully employed¹ as chiral auxiliaries and as chiral catalysts in many asymmetric syntheses. Among the 1,1'-bi-2-naphthol compounds, 3,3'-diphenyl-[2,2'-binaphthalene]-1,1'-diol (VANOL) was found² to be a very efficient catalyst for several reactions. The absolute configuration of (-)₅₈₉-VANOL has been determined³ from the X-ray structure of brucine binaphtholphosphate salt to be (aS), where (-)₅₈₉ represents

the sample of VANOL with negative optical rotation at 589 nm in either CH₂Cl₂ or THF solvent. This assignment has been widely used,² and commercial suppliers of VANOL have adopted this assignment. Unfortunately, the X-ray structure of what was then considered to have been the salt of (-)₅₈₉-(aS)-VANOL is now noted to contain (aR)-VANOL, which introduces uncertainty into the assigned absolute configuration of VANOL. In light of this observation, two questions arise: (1) Are the widely used absolute configuration assignments, (+)₅₈₉-(aR)-VANOL and (-)₅₈₉-(aS)-VANOL, correct? (2) If those assignments are correct, then what is the source of the discrepancy in the reported X-ray crystal structure? These questions are resolved in this manuscript.

To determine the absolute configuration and the magnitude of the dihedral angle around the axis connecting two naphthyl groups, X-ray diffraction has been the preferred approach in the past, if the compound of interest could be crystallized. Alternately, different solution-phase spectroscopic methods, including electronic circular dichroism (ECD) and NMR spectroscopy, have also been employed for this purpose. The absolute configurations of compounds containing binaphthyl groups have also been determined in

(1) Aydin, J.; Kumar, K. S.; Sayah, M. J.; Wallner, O. A.; Szabo, K. J. *J. Org. Chem.* **2007**, *72* (13), 4689–4697.

(2) (a) Yu, S.; Rabalakos, C.; Mitchell, W. D.; Wulff, W. D. *Org. Lett.* **2005**, *7* (3), 367–369. (b) Heller, D. P.; Goldberg, D. R.; Wulff, W. D. *J. Am. Chem. Soc.* **1997**, *119*, 10551–10552. (c) Heller, D. P.; Goldberg, D. R.; Wu, H.; Wulff, W. D. *Can. J. Chem.* **2006**, *84* (10), 1487–1503. (d) Xue, S.; Yu, S.; Deng, Y.; Wulff, W. D. *Angew. Chem., Int. Ed.* **2001**, *40* (12), 2271–2274. (e) Antilla, J. C.; Wulff, W. D. *J. Am. Chem. Soc.* **1999**, *121*, 5099–5100. (f) Antilla, J. C.; Wulff, W. D. *Angew. Chem., Int. Ed.* **2000**, *39* (24), 4518–4521. (g) Bolm, C.; Frison, J. C.; Zhang, Y.; Wulff, W. D. *Synlett* **2004**, 1619–1621. (h) Zhang, Y.; Desai, A.; Lu, Z.; Hu, G.; Ding, D.; Wulff, W. D. *Chem.—Eur. J.* **2008**, *14*, 3785–3803. (i) Zhang, Y.; Lu, Z.; Desai, A.; Wulff, W. D. *Org. Lett.* **2008**, *10*, 5429–5432.

(3) Bao, J.; Wulff, W. D.; Dominy, J. B.; Fumo, M. J.; Grant, E. B.; Rob, A. C.; Whitcomb, M. C.; Yeung, S.; Ostrander, R. L.; Rheingold, A. L. *J. Am. Chem. Soc.* **1996**, *118*, 3392–3405.

the past^{4–8} using exciton couplets associated with ¹B transitions in the ECD spectra.

In recent years, chiroptical spectroscopic methods have emerged⁹ as powerful tools to determine the absolute configuration and predominant conformations of chiral molecules in solution phase. The successful use of chiroptical spectroscopic methods depends on the reliable theoretical predictions of corresponding properties, and therefore reliable quantum chemical predictions of chiroptical properties are needed along with experimental measurements. These chiroptical spectroscopic methods include vibrational circular dichroism (VCD), vibrational Raman optical activity (VROA), electronic circular dichroism (ECD), and optical rotatory dispersion (ORD). While all four methods need not be used simultaneously, the use of more than one method certainly helps remove any uncertainty in the conclusions emerging from individual methods.¹⁰ Furthermore, as the sensitivity to conformational details varies among these methods, a complete understanding can only be obtained sometimes using multiple methods.

There are only a limited number of VCD studies on binaphthol compounds. Sugeta and co-workers¹¹ have measured the VCD in the O–H stretching region of 1,1'-bi-2-naphthol in different solvents and interpreted the observed spectra using coupled oscillator model. Urbanova and co-workers¹² measured the VCD in the mid-infrared region for 1,1'-bi-2-naphthol, 1,1'-bi-2-naphthol-3-carboxylic acid, and 1,1'-bi-2-naphthol-3-carboxylate and interpreted the observed spectra using quantum chemical predictions using BPW91 functional and 6-31G* basis set. Starting from 1,1'-bi-2-naphthol, a bisetherketone macrocycle was prepared by Cao et al., and its absolute configuration was determined¹³ using VCD spectroscopy. Recently, conformational sensitivity of 6,6'-dibromo-1,1'-bi-2-naphthol (DBBN) was investigated¹⁴ using VCD, ECD, and ORD spectroscopies. Although several papers^{4–8} in the literature dealt with interpreting the ECD spectra of binaphthol compounds using semiempirical methods, quantum chemical predictions of ECD were reported only for limited cases.¹⁴ Similarly, optical rotation at 589 nm is routinely reported by synthetic chemists whenever a compound is synthesized, but ORD data are not routinely reported. The experimental and quantum theoretical ORD spectra are also available only for a limited number of binaphthol compounds.¹⁴ It is of

TABLE 1. B3LYP/6-311G(2d,2p) Energies of Three Conformers of VANOL

conformer ^a	optimized energy (au)	relative energy (kcal/mol)
<i>cis-cis</i>	–1383.52393425	0
<i>cis-trans</i>	–1383.51662608	4.5
<i>trans-trans</i>	–1383.51047632	8.4

^a*cis-cis*: both dihedral angles H–O–C₁–C₂ and H–O–C₁'–C₂' are ~0°; *cis-trans*: dihedral angles H–O–C₁–C₂ and H–O–C₁'–C₂' are ~0° and 180° respectively; *trans-trans*: both dihedral angles H–O–C₁–C₂ and H–O–C₁'–C₂' are ~180°.

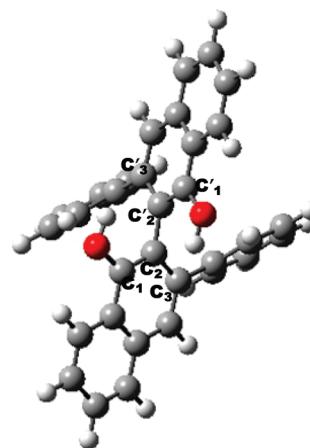


FIGURE 1. Optimized structure for *cis-cis* conformer of (aS)-3,3'-diphenyl-[2,2'-binaphthalene]-1,1'-diol, with pertinent atomic labels.

interest to note that VCD, ECD, and ORD spectroscopies have been used¹⁵ to confirm the absolute configuration of a related molecule, 2,2'-diphenyl-[3,3'-biphenanthrene]-4,4'-diol (VAPOL).

The latest developments in chiroptical spectroscopic methods⁹ can be used to establish the absolute configuration of VANOL. These developments include theoretical formalism¹⁶ and its subsequent implementation in the quantum chemical programs¹⁷ within the density functional framework for VCD. Additionally, following the first quantum chemical prediction of optical rotation,¹⁸ remarkable advances have taken place in the prediction of ORD using density functional and coupled cluster theories.¹⁹ Around the same time, density functional theoretical methods for ECD predictions²⁰ have appeared.

In this work, first we confirm the absolute configuration³ of VANOL as (–)₅₈₉-(aS) and (+)₅₈₉-(aR) using VCD, ECD,

(4) Mason, S. F.; Seal, R. H.; Roberts, D. R. *Tetrahedron* **1974**, *30*, 1671–1682.

(5) Rosini, C.; Rosati, I.; Spada, G. P. *Chirality* **1995**, *7*, 353–358.

(6) Bari, L. D.; Pescitelli, G.; Salvadori, P. *J. Am. Chem. Soc.* **1999**, *121*, 7998–8004.

(7) Proni, G.; Spada, G. P.; Lustenberger, P.; Welti, R.; Diedrich, F. J. *Org. Chem.* **2000**, *65*, 5522–5527.

(8) Superchi, S.; Giorgio, E.; Rosini, C. *Chirality* **2004**, *16*, 422–451.

(9) For recent reviews see: (a) Bringmann, G.; Bruhn, T.; Maksimenka, K.; Hemberger, Y. *Eur. J. Org. Chem.* **2009**, 2717–2727. (b) Nafie, L. A. *Nat. Prod. Commun.* **2008**, *3*, 451–466. (c) Berova, N.; Di Bari, L.; Pescitelli, G. *Chem. Soc. Rev.* **2007**, *36*, 914–931. (d) Polavarapu, P. L. *Chem. Rec.* **2007**, *7*, 125–136. (e) Barron, L. D.; Hecht, L.; McColl, I. H.; Blanch, E. W. *Mol. Phys.* **2004**, *102*, 731–744.

(10) Polavarapu, P. L. *Chirality* **2008**, *20* (5), 664–72.

(11) Nakao, K.; Kyogoku, Y.; Sugeta, H. *Faraday Discuss.* **1994**, *99*, 77–85.

(12) Setnicka, V.; Urbanova, M.; Bour, P.; Kral, V.; Volka, K. *J. Phys. Chem. A* **2001**, *105*, 8931–8938.

(13) Cao, H.; Ben, T.; Su, Z. M.; Zhang, M.; Kan, Y. H.; Yan, X.; Zhang, W. J.; Wei, Y. *Macromol. Chem. Phys.* **2005**, *206*, 1140–1145.

(14) Polavarapu, P. L.; Jeirath, N.; Walia, S. *J. Phys. Chem.* **2009**, *3*, 5423–5431.

(15) Petrovic, A. G.; Vick, S. E.; Polavarapu, P. L. *Chirality* **2008**, *20*, 501–510.

(16) (a) Galwas, P. A. Ph.D. Thesis, University of Cambridge, Cambridge, 1983. (b) Buckingham, A. D.; Fowler, P. W.; Galwas, P. A. *Chem. Phys.* **1987**, *112*, 1–14. (c) Stephens, P. J. *J. Phys. Chem.* **1985**, *89*, 748–752.

(17) (a) Gaussian 03, www.gaussian.com. (b) Turbomole, www.turbomole.com. (c) Amsterdam Density functional program, www.scm.com. (d) Dalton program, www.kjemi.uio.no/software/dalton/. (e) PSI 3.2, www.psi-code.org

(18) Polavarapu, P. L. *Mol. Phys.* **1997**, *91*, 551–554.

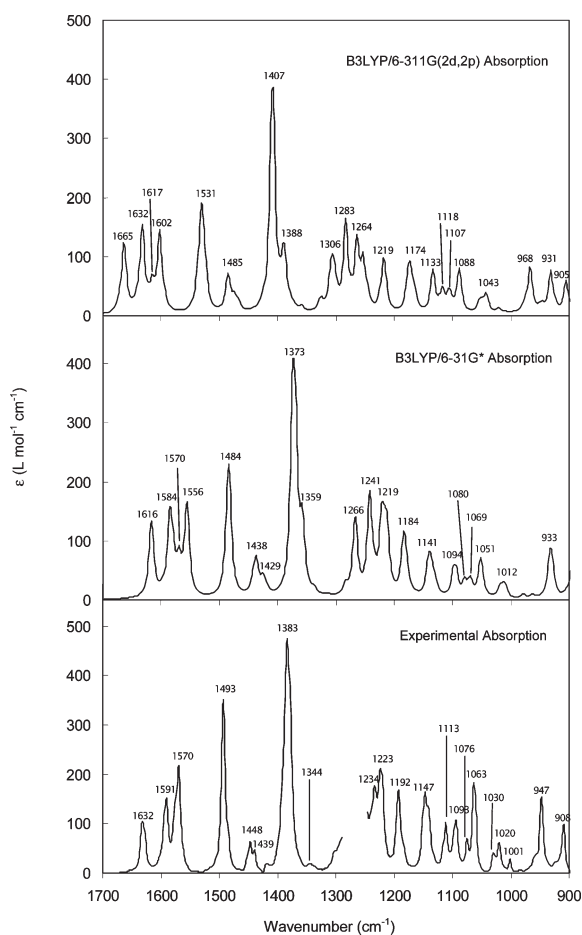
(19) For recent reviews, see: (a) Autschbach, J. *Comp. Lett.* **2007**, *3*, 131–150. (b) Crawford, T. D. *Theor. Chem. Acc.* **2006**, *115* (4), 227–245. (c) Polavarapu, P. L. *Chirality* **2002**, *14*, 768–781; **2003**, *15*, 284–285.

(20) (a) Pecul, M.; Ruud, K.; Helgaker, T. *Chem. Phys. Lett.* **2004**, *388*, 110–119. (b) Stephens, P. J.; McCann, D. M.; Devlin, F. J.; Cheeseman, J. R.; Frisch, M. J. *J. Am. Chem. Soc.* **2004**, *126*, 7514–7521. (c) Diedrich, C.; Grimme, S. *J. Phys. Chem. A* **2003**, *107*, 2524–2539. (d) Autschbach, J.; Ziegler, J. T.; van Gisbergen, S. J. A.; Baerends, E. J. *J. Chem. Phys.* **2002**, *116*, 6930–6940.

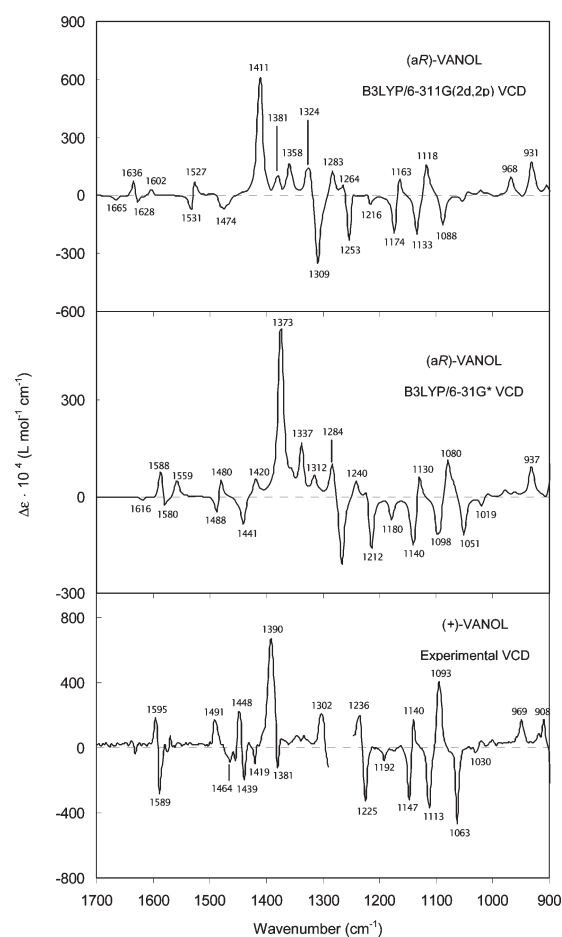
TABLE 2. Selected Dihedral Angles and Bond Lengths of (a*S*)-3,3'-Diphenyl-[2,2'-binaphthalene]-1,1'-diol

parameter ^{a,b}	B3LYP/6311G (2d,2p)	literature crystal geometry ^c	new crystal geometry ^d
C _{ph2} -C _{ph1} -	58	-47	+51
C ₃ -C ₂			
C ₁ -C ₂ -C ₂ '-	81	-49	+42
C ₁ '			
H-O-C ₁ -C ₂	-2.0		
C-O	1.36	1.39	1.39
C ₂ -C ₂ '	1.49	1.51	1.49

^aC₁ and C₁' are carbon atoms of naphthyl groups to which hydroxyl groups are attached; C₂ and C₂' are carbon atoms connecting two naphthyl groups; C₃ and C₃' are carbon atoms of naphthyl groups to which phenyl groups are attached; C_{ph1} is the carbon atom of phenyl group attached at C₃ and C_{ph2} is the adjacent carbon atom of same phenyl group that is closest to C₂. ^bBond lengths in Å, and bond angles in degrees. ^cThe dihedral angles in crystal structure have opposite signs because the coordinates in the supplementary data of ref 3 have (a*R*)-structure. ^dNew crystal structure determined in this study; see text.

**FIGURE 2.** Comparison of experimental absorption spectra (bottom trace) with those predicted at B3LYP/6-31G* and B3LYP/6-311G(2d,2p) levels for VANOL. The predicted traces have been simulated using Lorentzian band shapes with 5 cm⁻¹ half-width at one-half of the peak height. The 6-31G* predicted vibrational frequencies were scaled by 0.9613. The experimental spectra were measured at a concentration of 0.114 M in CH₂Cl₂ solvent and 145 μm path length.

and ORD spectroscopies. Then the discrepancy in the previously reported³ crystal structure is resolved by undertaking new investigations on the diastereomeric salts of (a*R*)- and

**FIGURE 3.** Comparison of experimental VCD spectra (bottom trace) of (+)-VANOL with those predicted for (a*R*)-VANOL at B3LYP/6-31G* and B3LYP/6-311G(2d,2p) levels. The predicted traces have been simulated using Lorentzian band shapes with 5 cm⁻¹ half-width at one-half of the peak height. The 6-31G* predicted vibrational frequencies were scaled by 0.9613. The experimental spectra were measured at a concentration of 0.114 M in CH₂Cl₂ solvent and 145 μm path length.

(a*S*)-VANOL with brucine and with the determination of the crystal structure of the dextrorotatory salt.

Results and Discussion

The conformational mobility of the hydroxyl groups in 1,1'-bi-2-naphthol compounds results in three different conformations.²¹ Designating C₁ and C₁' as representing the carbon atoms to which hydroxyl groups are attached and C₂ and C₂' as adjacent carbon atoms that connect the two binaphthyl groups, these conformations have (a) *cis-cis* orientation where H-O-C₁-C₂ and H-O-C₁'-C₂' are each in *cis* orientation (dihedral angle ~0°); (b) *cis-trans* orientation where H-O-C₁-C₂ and H-O-C₁'-C₂' are in *cis* (dihedral angle ~0°) and *trans* (dihedral angle ~180°) orientations; and (c) *trans-trans* orientation where H-O-C₁-C₂ and H-O-C₁'-C₂' are in *trans* (dihedral angle ~180°) and *trans* (dihedral angle ~180°) orientations. The energies of these three conformers of VANOL predicted at B3LYP/6-311G(2d,2p) level are compared in Table 1.

(21) Sahnoun, R.; Koseki, S.; Fujimura, Y. *J. Mol. Struct.* **2005**, 735–736, 315–324.

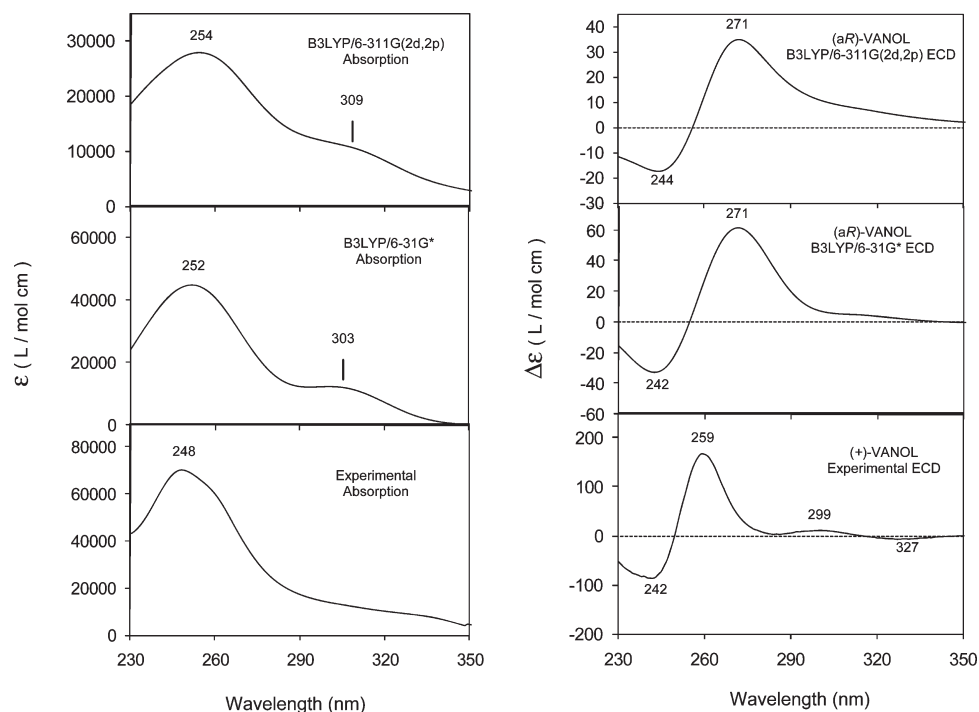


FIGURE 4. Comparison of experimental (bottom) and theoretical electronic absorption (left panel) and ECD (right panel) spectra for VANOL. Theoretical ECD spectrum for (aR)-VANOL was simulated using Lorentzian band shapes with 10 nm half-width at one-half of the peak height. The experimental spectra were measured at a concentration of 1.4×10^{-3} M in CH_2Cl_2 solvent and 0.01 cm path length.

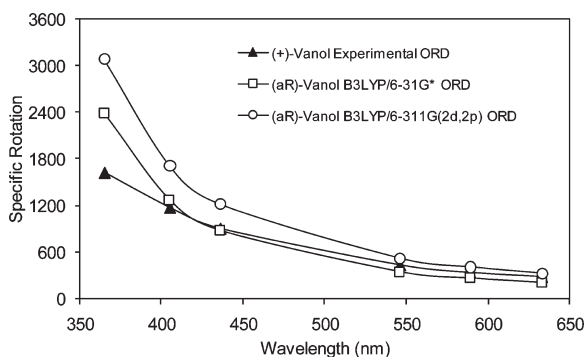


FIGURE 5. Comparison of experimental ORD data of (+)-VANOL with ORD predicted for (aR)-VANOL at B3LYP/6-31G* and B3LYP/6-311G(2d,2p) levels. The measurements were done at a concentration of 0.5 mg/mL in CH_2Cl_2 solvent and 1 dm path length.

The *cis-cis* conformer (Figure 1) is of lowest energy for the isolated molecule, and the *cis-trans* and *trans-trans* conformations are, respectively, ~ 4.5 and ~ 8.4 kcal/mol higher in energy. The same trend was found for 6,6'-dibromo-1,1'-bi-2-naphthol and for 1,1'-bi-2-naphthol. Because of the large energy difference among the three conformers, the *cis-trans* and *trans-trans* conformers are unlikely to be dominant in non-hydrogen bonding solvents.¹⁴

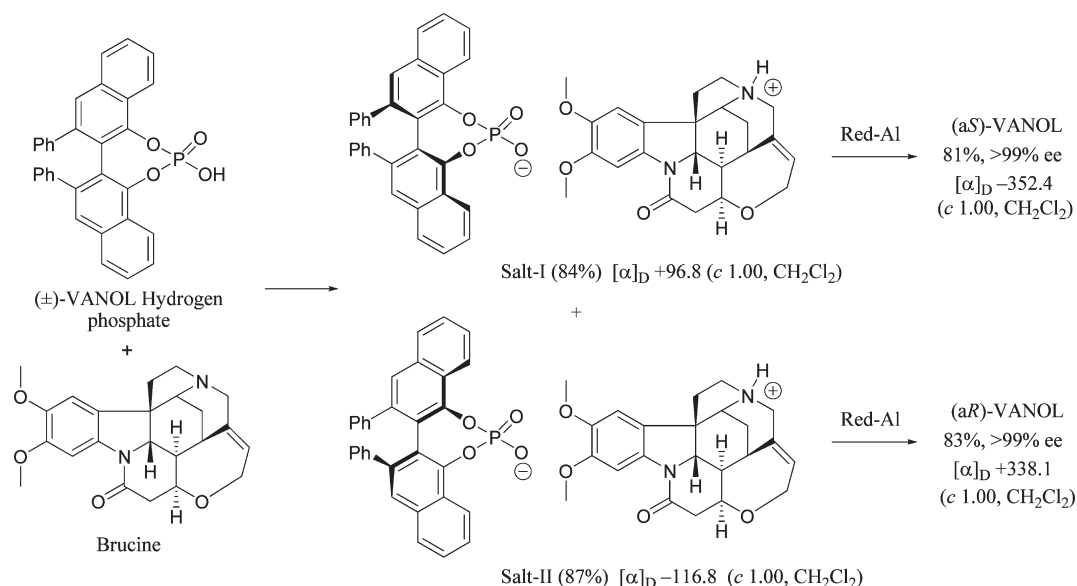
Selected structural parameters obtained from the B3LYP/6-311G(2d,2p) optimized structures are compared to those of crystal structure³ in Table 2. The crystal structure was not determined directly for VANOL, but instead chemically modified brucinebinaphtholphosphate complex was used. In brucinebinaphtholphosphate complex, hydroxyl hydrogen atoms are not present and the two oxygen atoms at 1 and

1' positions became part of the phosphate group. As a result, the structural parameters cannot be directly compared between isolated molecule and crystal structures. Even in the absence of any chemical modifications, the crystal structures can be expected to be different²² from the isolated molecular structures. The two naphthol groups are oriented at 81° in the isolated molecule, whereas those in the crystal structure are oriented at 49° . Similarly the phenyl group is oriented at 58° to the binaphthyl group in the isolated molecule and at 47° in the crystal structure. Note that the coordinates provided in the supplementary data of ref 3 have (aR) structure and therefore the dihedral angles (Table 1) obtained from the crystal structure of ref 3 have signs opposite to those of the isolated molecule with (aS) configuration.

The experimental vibrational absorption spectrum in the $1700\text{--}900\text{ cm}^{-1}$ region is compared to the corresponding predicted spectrum in Figure 2. This mid-infrared region is dense with numerous vibrational bands, just as expected for molecules containing binaphthyl groups. One-to-one correspondence can be seen for a majority of the bands between experimental and theoretical absorption spectra. Although there are differences in relative intensities among some experimental and predicted absorption bands, which are unavoidable for the lack of solvent influence in theoretical predictions, the overall qualitative correlation is remarkably good. As the absorption spectra are sensitive to the conformation, the qualitatively satisfactory agreement seen among experimental and predicted vibrational absorption spectra can be used to suggest that the conformation used for the calculations is probably close to that adopted by VANOL in CH_2Cl_2 solvent.

(22) Wang, F.; Polavarapu, P. L.; Drabowicz, J.; Kielbasinski, P.; Potrzebowski, M. J.; Mikolajczyk, M.; Wieczorek, M. W.; Majzner, W. W.; Lazewska, I. *J. Phys. Chem.* **2004**, *108*, 2072–2079.

SCHEME 1



The assignment of absolute configuration depends on a satisfactory comparison between experimental and calculated VCD spectra. The predicted VCD spectrum for (aR)-VANOL is compared to the experimental VCD spectrum of (+)-VANOL in Figure 3. One-to-one sign correspondence and good paralleling of relative intensities between the experimental and theoretical VCD bands can be clearly seen. This satisfactory correlation among the VCD signals in experimental and predicted spectra leads to an unambiguous assignment that the (aR)-configuration corresponds to the (+)₅₈₉-VANOL.

The experimental electronic absorption spectrum of VANOL (Figure 4) exhibits a weak broad absorption band at 320 nm and a band with strong absorption intensity at ~248 nm. The 248 nm experimental band also shows an unresolved long wavelength shoulder at ~260 nm. These features, except for the one corresponding to the experimental shoulder band at 260 nm, are also present in the predicted electronic absorption spectra.

The ECD spectrum of (+)-VANOL (Figure 4) exhibits a positive band at 259 nm and a negative band at 242 nm. Both B3LYP/6-31G* and B3LYP/6-311G(2d,2p) predicted ECD spectra for (aR)-VANOL reproduce these observed ECD bands, as can be seen in Figure 4. This correlation provides another independent verification of the absolute configuration of VANOL as (+)₅₈₉-(aR).

As a third verification of the configurational assignment, the experimental ORD data of (+)-VANOL have been compared to the predicted ORD of (aR)-VANOL in Figure 5. In principle, the wavelengths used for ORD predictions should be shifted²³ from those used for experimental ORD measurements because the predicted electronic transition wavelengths generally appear at longer wavelengths²⁴ than those experimentally observed. However, no attempt has been made here to correct for the transition wavelength differences as these differences between predicted and observed transition

wavelengths do not influence the conclusions here. This is because the predicted ORD for (aR)-VANOL and experimental ORD of (+)-VANOL are both monosignate at all wavelengths investigated and these ORD spectra can be shifted along wavelength scale as a whole relative to each other without influencing any conclusions derived here. There is a satisfactory agreement between the experimental specific rotations for the (+)-enantiomer and the corresponding values for (aR)-VANOL. This agreement in the signs of optical rotation and the trend in ORD spectra (increasingly positive at shorter wavelengths) support the conclusions about absolute configuration derived from VCD and ECD data. Thus all three chiroptical spectroscopic methods suggest that the absolute configuration of VANOL is (+)₅₈₉-(aR), which is in agreement with the assignment established before.³

However, the reported crystal structure,³ which was thought to have contained brucine salt of (aS)-VANOL, actually contained (aR)-VANOL. This observation introduces a discrepancy between the configuration just established and the crystal structure. To resolve this discrepancy, the structures of the diastereomeric salts formed in the reaction of racemic VANOL hydrogenphosphate and brucine have been reinvestigated (Scheme 1).

The hydrogenphosphate ester of racemic VANOL was prepared as previously described.³ It was found that when attempts were made to selectively crystallize one of the salts from the mixture, either the levorotatory salt or the dextrorotatory salt could be induced to be the first to crystallize depending on the choice of solvents. With 1,2-dichloroethane as solvent, the levorotatory salt (Salt II) came out first, and with ethanol the dextrorotatory salt (Salt I) came out first. However, the purity of the salts that were obtained by crystallization was highest when the Salt II was crystallized first. Thus, crystallization of the mixture of salts prepared from racemic VANOL hydrogenphosphate from 1,2-dichloroethane gave Salt II in 87% yield (based on the amount of (aR)-enantiomer in racemic VANOL) with > 99% purity and with an optical rotation of -116.8° . The mother liquor was stripped of volatiles, and the residue

(23) Polavarapu, P. L. *J. Phys. Chem. A* **2005**, *109*, 7013–7023.

(24) Bauernschmitt, R.; Ahlrichs, R. *Chem. Phys. Lett.* **1996**, *256*, 454–464.

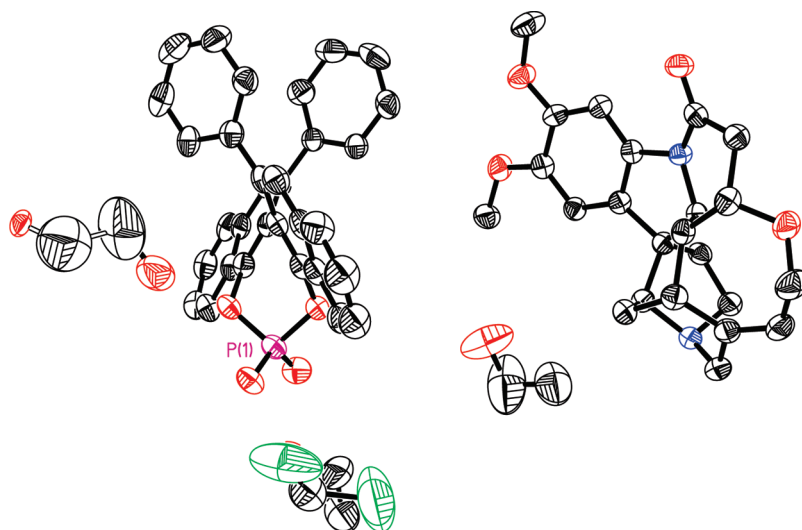


FIGURE 6. ORTEP drawing of the dextrorotatory brucine salt of (a*S*)-VANOL Hydrogenphosphate with 50% ellipsoids. One ethanol molecule is disordered.

crystallized from a 10:1 mixture of ethanol and 1,2-dichloroethane to give Salt I in 84% yield (based on the amount of (a*S*)-enantiomer in racemic VANOL) with >99% purity and with an optical rotation of +96.8. Optically pure (a*S*)- or (a*R*)-VANOL could be liberated from these salts by reduction with Red-Al, and in each case the optical purity was >99% ee as determined by HPLC with a Pirkle phenylglycine column.³ The dextrorotatory salt gave (a*S*)-VANOL in 81% yield and an optical rotation of -352.4° . The levorotatory salt gave (a*R*)-VANOL in 83% yield and an optical rotation of $+338.1^\circ$. A crystal of Salt I was taken for X-ray analysis from a sample that was shown to be >99% pure and free of Salt II by reduction to (a*S*)-VANOL, and it was determined that the optical purity of (a*S*)-VANOL was greater than 99% ee. This crystal structure was determined as described in the Experimental Section and revealed that the dextrorotatory salt is formed from VANOL that has an (a*S*)-configuration. This structure is shown in Figure 6. One ethanol molecule is disordered.

It is not clear what the source of the error was in our original publication.³ It may have been that samples of the two salts were mislabeled or that the sample of the dextrorotatory salt that we subjected to crystallization was not pure and crystals of the levorotatory salt were picked out for analysis.

Conclusion

The comparison between experimental and predicted spectral data associated with VCD, ECD, and ORD have indicated that the (a*R*)-configuration belongs to the (+)₅₈₉-enantiomer of VANOL and therefore the (a*S*)-configuration belongs to the (–)₅₈₉-enantiomer. This assignment is consistent with the new X-ray crystal structure data obtained for the brucine binaphtholphosphate salt of the (a*S*)-enantiomer of VANOL.

Experimental Section

Calculations. All calculations were undertaken with the Gaussian program suite^{17a} using B3LYP functional and 6-31G* and 6-311G(2d,2p) basis sets. The geometries of three

conformers of VANOL with (a*S*)-configuration were fully optimized. The optimized geometry for *cis-cis* conformer (Figure 1) was used for predicting VCD, ECD, and ORD properties. From the calculated vibrational frequencies, the *cis-cis* conformation considered was found to represent the minima on the potential energy surface, as there are no imaginary frequencies. To obtain VCD, ECD, and ORD properties for the (a*R*) configuration, those obtained for (a*S*) configuration were multiplied by -1 .

The theoretical absorption and VCD spectra (Figures 2 and 3) were simulated with Lorentzian band shapes and 5 cm^{-1} half-width at half-peak height. The 6-31G* predicted vibrational band positions are normally higher than the experimental vibrational band positions, and therefore the 6-31G* calculated frequencies have been scaled by a factor of 0.9613. No such scaling was used for 6-311G(2d,2p) predicted vibrational frequencies. The theoretical ECD spectra (Figure 4) were simulated using Lorentzian band shapes and 20 nm half-width at half-peak height. The predicted electronic transition wavelengths are used as such without any scaling. The electronic absorption spectra (Figure 4) are presented as molar extinction coefficient (in L/mol/cm), derived from dimensionless oscillator strength. The peak extinction coefficient of *i*th band, ϵ_i^0 , is related to oscillator strength, f_i , as $\epsilon_i^0 = 7.369f_i(\lambda_i^2)/(\Delta_i)$, where Δ_i is the half-width at half-height of Lorentzian band.

Measurements. For VCD, ECD, and ORD measurements, commercial samples of both enantiomers of VANOL have been used as received. The absorption and VCD spectra were recorded in the $2000\text{--}900\text{ cm}^{-1}$ region. The VCD spectra were recorded with 1-h data collection time at 4 cm^{-1} resolution. Spectra were measured in CH_2Cl_2 solvent at 0.114 M concentration for (–)- and (+)-enantiomers. The sample was held in a variable path length cell with BaF_2 windows and a path length of $145\text{ }\mu\text{m}$. In the absorption spectrum presented (Figure 2), the solvent absorption was subtracted out and the region $\sim 1294\text{--}1248\text{ cm}^{-1}$ has been removed from experimental traces due to interference from strong solvent absorption. Since the region blocked from solvent absorption is very small, no attempts were made to measure the spectra in CD_2Cl_2 solvent. The VCD spectrum presented here (Figure 3) is obtained as the difference between the VCD spectra of enantiomers and the result is multiplied by 0.5. Concentration-dependent infrared absorption spectral measurements for a related molecule,¹⁴ 6,6'-dibromo-1,1'-bi-2-naphthol, did not indicate any aggregation.

The electronic absorption (EA) and electronic circular dichroism (ECD) spectra (Figure 4) were recorded at a concentration of 1.4×10^{-3} M in CH_2Cl_2 using 0.01 cm path length quartz cell. The optical rotations at five discrete wavelengths (633, 589, 546, 436, 405 nm) have been measured (Figure 5) at a concentration of 0.5 mg/mL in CH_2Cl_2 solvent using 1 dm cell. The optical rotations are expected¹⁴ to be different in DMSO solvent due to intermolecular hydrogen bonding with that solvent.

Preparation of the Levo- and Dextrorotatory Salts of VANOL Hydrogen Phosphate and Brucine. Freshly prepared (\pm)-VANOL hydrogen phosphate³ (45.2 g, 90.3 mmol) was placed in a 500 mL 3-neck round-bottom flask that was equipped with a condenser and a stir bar, that had been flushed with a nitrogen stream that was introduced via a needle in a septum on one of the necks of the flask, and that was monitored by a bubbler attached to the condenser. To the flask was added 1,2-dichloroethane (200 mL), and the contents of the flask were stirred and brought to a boil by heating the flask with a heating mantle. To a separate 250 mL pear-shaped flask was added brucine dihydrate (38.0 g, 88.6 mmol, technical grade, 92.6%) and 90 mL of 1,2-dichloroethane. The content of the flask was purged with nitrogen for about 2 min, and then the flask was sealed with a rubber septum that was fitted with a nitrogen balloon. This flask was heated by swirling in hot flowing water (50 °C) until a clear colorless solution (volume about 110 mL) resulted, which had a small amount of a gray insoluble impurities floating on top. The resulting solution was placed in a hot water bath (50 °C), and 60 mL of the brucine solution was removed by a syringe equipped with a 12 gauge needle and added to the solution of VANOL hydrogen phosphate over a period of about 1 min to give a brownish clear solution. The remainder of the brucine solution (about 50 mL) was loaded into the syringe, leaving the insoluble material in the flask. The brucine solution was slowly added via syringe pump (addition rate 100 mL/h). Solid began to form when about 22 mL of the solution was left in the syringe. The addition was paused while the suspension was refluxed for 15 min, and then the addition was resumed to complete the addition to the suspension. An additional portion of 1,2-dichloroethane (10 mL) was used to rinse the pear flask, leaving the insoluble material (1.7 g) in the flask. The final washing was added over a period of 1 min. The resulting suspension was cooled slowly to room temperature and then left undisturbed for 48 h. The white solid was collected by filtration through a Büchner funnel, washed three times with 1,2-dichloroethane (25 mL), and then dried over high vacuum for 12 h to afford 36.28 g (40.5 mmol) of Salt II with the following specific rotation: $[\alpha]_{\text{D}} -116.8$ (*c* 1.00, CH_2Cl_2). A small sample of Salt II was reduced to give (a*R*)-VANOL, which was found to be >99% ee and have the following specific rotation: $[\alpha]_{\text{D}} +338.1$ (*c* 1.00, CH_2Cl_2).³

The dark yellow mother liquor was stripped of volatiles by rotary evaporator and combined with 100 mL of $\text{ClCH}_2\text{CH}_2\text{Cl}$ in a 2 L 1-neck round-bottom flask fitted with a condenser. The resulting mixture was stirred and brought to a boil to dissolve the solid residue. A total of 1000 mL of ethanol was added in portions as follows. First 300 mL of ethanol was added and the resulting solution was returned to a boil, and then an additional 200 mL of ethanol was added and the mixture again returned to a boil. At this point another 200 mL portion of ethanol was added, and the mixture was refluxed for 15 min until it appeared that no further accumulation of precipitate was occurring. Finally, an additional 300 mL portion of ethanol was then added, and the mixture was refluxed for 10 min before being allowed to cool to room temperature and stand undisturbed overnight. The beige solid was isolated by filtration in a Büchner funnel and dried over high vacuum for 12 h to afford 34.82 g (38.9 mmol) of salt I which had the following specific rotation:

$[\alpha]_{\text{D}} +96.8$ (*c* 1.00, CH_2Cl_2). A small sample of Salt I was reduced to give (a*S*)-VANOL which was found to be >99% ee and have the following specific rotation: $[\alpha]_{\text{D}} -352.4$ (*c* 1.00, CH_2Cl_2).³

X-ray Data. An X-ray diffraction analysis was carried out on a crystal obtained from the dextrorotatory salt obtained from racemic VANOL Hydrogen phosphate and brucine. A colorless block crystal with dimensions 0.56 mm \times 0.51 mm \times 0.39 mm was mounted on a nylon loop using a very small amount of paratone oil.

Data were collected using a CCD (charge coupled device) based diffractometer equipped with a low-temperature apparatus operating at 173 K. Data were measured using ω and ϕ scans of 0.5° per frame for 30 s. The total number of images was based on results from the program COSMO²⁵ where redundancy was expected to be 4.0 and completeness to 0.83 Å to 100%. Cell parameters were retrieved using APEX II software²⁶ and refined using SAINT on all observed reflections. Data reduction was performed using the SAINT software,²⁷ which corrects for Lp. Scaling and absorption corrections were applied using SADABS²⁸ multiscan technique, supplied by George Sheldrick. The structures are solved by the direct method using the SHELXS-97 program and refined by least-squares method on F^2 , SHELXL-97, which are incorporated in SHELXTL-PC V 6.10.²⁹

The structure was solved in the space group $P2_12_12_1$ (No. 19). All non-hydrogen atoms are refined anisotropically. Hydrogens were calculated by geometrical methods and refined as a riding model. The Flack³⁰ parameter is used to determine chirality of the crystal studied (the value should be near zero; a value of one indicates the other enantiomer and a value of 0.5 indicates racemic). The Flack parameter was refined to 0.03(3), confirming the absolute stereochemistry. Determination of absolute structure using Bayesian statistics on Bijvoet differences using the program within Platon³¹ also report that we have the correct enantiomer based on this comparison.³² All drawings are done at 50% ellipsoids.

Acknowledgment. Some of the calculations utilized the NCSA IBM P690 system, partially supported by the National Center for Supercomputing Applications under TG-CHE060063T. A teaching assistantship from Vanderbilt University (to A.G.P.) is greatly appreciated. The CCD based X-ray diffractometers at Michigan State University were upgraded and/or replaced by departmental funds.

Supporting Information Available: X-ray structure data for the dextrorotatory salt from (\pm)-VANOL hydrogen phosphate and brucine; Cartesian coordinates for optimized geometry; table of vibrational absorption intensities and rotational strengths; table of electronic oscillator rotational strengths. This material is available free of charge via the Internet at <http://pubs.acs.org>.

(25) COSMO V1.56, Software for the CCD Detector Systems for Determining Data Collection Parameters; Bruker Analytical X-ray Systems: Madison, WI, 2006.

(26) APEX2 V 1.2-0, Software for the CCD Detector System; Bruker Analytical X-ray Systems: Madison, WI, 2006.

(27) SAINT V 7.34, Software for the Integration of CCD Detector System; Bruker Analytical X-ray Systems: Madison, WI, 2001.

(28) Blessing, R. H. SADABS V2.10, Program for absorption corrections using Bruker-AXS CCD based on the method of Robert Blessing. *Acta Crystallogr.* **1995**, *A51*, 33–38.

(29) Sheldrick, G. M. *Acta Crystallogr.* **2008**, *A64*, 112–122.

(30) Flack, H. D. *Acta Crystallogr.* **1983**, *A39*, 876–881.

(31) Spek, A. L. *J. Appl. Crystallogr.* **2003**, *36*, 7–13.

(32) Hooft, R. W. W.; Straver, L. H.; Spek, A. L. *J. Appl. Crystallogr.* **2008**, *41*, 96–103.